CONTROL OF TWO INDUCTION MOTORS FED BY A FIVE-PHASE VOLTAGE-SOURCE INVERTER

Bruno Francois, Bouscayrol Alain

Electrimacs'99 ISBN 972-98257-0-X

CONTROL OF TWO INDUCTION MOTORS FED BY A FIVE-PHASE VOLTAGE-SOURCE INVERTER

François B. [1], Bouscayrol A.[2]

[1] L2EP, E.C. Lille, Cité Scientifique BP48, 59651 Villeneuve d'Ascq, France
tel: 3 20 33 54 59, fax: 3 20 33 54 54, e_mail: francois@ec-lille.fr
[2] L2EP, U.S.T.L., 59655 Villeneuve d'Ascq, France

Abstract: This paper deals with a dynamic control of two induction motors supplied by a common five-phase power inverter. A complete formulation of the system and a control design procedure are presented. The inverter control is specially detailed because of its complexity. The proposed strategy allows independent controls of both induction machines. Simulation results on 2kW induction machines validate the theoretical considerations.

1.- INTRODUCTION

Nowadays, multi machines systems are more and more used in industrial applications [1] [2]. Often, induction machines are chosen for their low cost and their dynamic performances with adapted controls [3]. In the standard case, each machine is supplied by a three-phase inverter. Recently new structures have been proposed, as four-phase inverters for two induction machines [4]. Advances include reduced power components, reduced auxiliary electronic components, reduced volume and weight of the overall power converter. Robotic and spatial applications are directly concerned by these advantages. The power structure of such multi-phase inverters is based on parallel connections of elementary commutation cells and common phases are used to supply several ac machines. However, because of the sharing of inverter phases, the machine control remains a critical point.

In this paper, the studied power structure is composed of two induction machines supplied by a five-phase power inverter (fig. 1). Two measured speeds and two estimated fluxes constitute the system outputs, which may be variables by modifying the magnitude, shift and frequency of the four inverter phase to phase voltages. These ones are obtained by creating four potential differences in comparison with one common commutation cell, which is then connected to both motors. An inverter controller has been designed to generate two independent systems of three voltages in order to get an independent control of the torques and the fluxes of both induction machines. The aim of this paper is to describe the control design procedure.

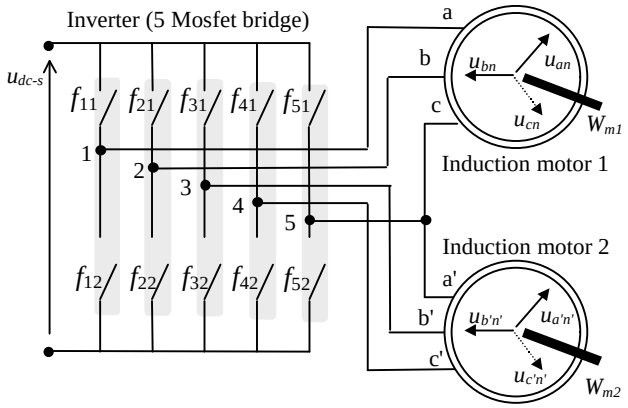

Fig. 1: Structure of the five-phase voltage-source inverter

This paper will be organized as follows. In section 2, the mathematical modelling of the enlarged inverter is presented with a causal input output graph of the global system. Section 3 is devoted to the design of the power system control by inversion of the mathematical modelling and is decomposed in a serial assembling of elementary control functions. In the inverter control part, non-linear functions and possible optimization tasks are explained. Attention is focused to the decoupling method of both sets of voltage supply. Simulation results are presented in section 4.

2.- ANALYSIS OF THE FIVE PHASE INVERTER BI - MACHINE SYSTEM

2.1.- Mathematical description

Each bi-directional switch blocks or conducts the current in both directions, depending on their gate control signal. Boolean switch states are written f_{cl} :

closed switch -> $f_{cl} = 1$

opened switch -> $f_{cl} = 0$ (1)

where $c \in \{1,2,3,4,5\}$ is the n° of the commutation cell and $l \in \{1,2\}$ is the n° of the switch. None of switch in a column connected to one voltage source may conduct

simultaneously to avoid short circuits. Moreover, in order to keep paths of all currents, at least one switch in a row must be opened. Therefore, only one switch must be closed in a column, which constitutes a commutation cell:

$$f_{c1} + f_{c2} = 1 \quad (2)$$

In consequence, only 2^5 states of the switching matrix must be considered (table 1). These states induce particular modulated voltages which are linked to the d.c. source voltage $u_{dc\text{-}s}$ as:

$$\begin{bmatrix} u_{15m} \\ u_{25m} \\ u_{35m} \\ u_{45m} \end{bmatrix} = \begin{bmatrix} m_1 \\ m_2 \\ m_3 \\ m_4 \end{bmatrix} u_{dc\text{-}s} \quad (3)$$

This relation makes appear three-level functions which are defined as conversion functions:

$$m_c = f_{c1} - f_{51} \quad (4)$$

where $m_c \in \{-1, 0, 1\}$.

Table 1: connection and conversion function values

Patterns	f_{11}	f_{21}	f_{31}	f_{41}	f_{51}	m_1	m_2	m_3	m_4
1	0	0	0	0	0	0	0	0	0
2	0	0	0	0	1	-1	-1	-1	-1
3	0	0	0	1	0	0	0	1	0
4	0	0	0	1	1	-1	-1	-1	0
5	0	0	1	0	0	0	0	1	0
6	0	0	1	0	1	-1	-1	0	-1
7	0	0	1	1	0	0	0	1	1
8	0	0	1	1	1	-1	-1	0	0
9	0	1	0	0	0	0	1	0	0
10	0	1	0	0	1	-1	0	-1	-1
11	0	1	0	1	0	0	1	0	1
12	0	1	0	1	1	-1	0	-1	0
13	0	1	1	0	0	0	1	1	0
14	0	1	1	0	1	-1	0	0	-1
15	0	1	1	1	0	0	1	1	1
16	0	1	1	1	1	-1	0	0	0
17	1	0	0	0	0	1	0	0	0
18	1	0	0	0	1	0	-1	-1	-1
19	1	0	0	1	0	1	0	0	1
20	1	0	0	1	1	0	-1	-1	0
21	1	0	1	0	0	1	0	1	0
22	1	0	1	0	1	0	-1	0	-1
23	1	0	1	1	0	1	0	1	1
24	1	0	1	1	1	0	-1	0	0
25	1	1	0	0	0	1	1	0	0
26	1	1	0	0	1	0	0	-1	-1
27	1	1	0	1	0	1	1	0	1
28	1	1	0	1	1	0	0	-1	0
29	1	1	1	0	0	1	1	1	0
30	1	1	1	0	1	0	0	0	-1
31	1	1	1	1	0	1	1	1	1
32	1	1	1	1	1	0	0	0	0

If winding voltages are assumed to be balanced, it is easy to find that they are linked to modulated voltages as:

$$\begin{bmatrix} u_{an} \\ u_{bn} \end{bmatrix} = \frac{1}{3} \begin{bmatrix} 2 & -1 \\ -1 & 2 \end{bmatrix} \begin{bmatrix} u_{15m} \\ u_{25m} \end{bmatrix} \quad (5)$$

$$\begin{bmatrix} u_{a'n'} \\ u_{b'n'} \end{bmatrix} = \frac{1}{3} \begin{bmatrix} 2 & -1 \\ -1 & 2 \end{bmatrix} \begin{bmatrix} u_{35m} \\ u_{45m} \end{bmatrix} \quad (6)$$

2.2.- Causal input output graph of the system

A graphical representation of the global system modelling is obtained by using the Causal Input Output Graph (CIOG) [5]. The relations are represented by balloons. A causal relation which depends on time contains an unidirectional arrow. A non-causal relation which has no time dependence contain bi-directional arrows. The CIOG of the global system points out a partitioning of the converter model into causality ordered subsystems [6]. The resulting subsystems are input-output reachable as well as structurally controllable, so that a " piece by piece " design of their corresponding control units can be accomplished (fig. 2).

The five switching functions of the commutation cells, f_{cl} lead to four modulated voltages u_{c5m}. The classical induction machine modelling is based on the knowledge of winding voltages. So, the voltage transformation due to the particular connection of the enlarged inverter to the ac machine windings is expressed by a relation which links modulated voltages to winding voltages, u_{jn}. Both winding voltages of an induction machine impose its flux F_r and its mechanical speed W_m. Remember that a flux control is needed to obtain good dynamic performances and, therefore, fluxes will be estimated $F_{r\text{-}est}$ from the stator current measurement $I_{s\text{-}mes}$.

3.- CONTROL OF THE FIVE-PHASE INVERTER

3.1.- Control of the global power system

In order to obtain a decoupled control of induction motors, both winding voltage systems (u_{an}, u_{bn}) and ($u_{a'n'}$, $u_{b'n'}$) must be set equal to both winding voltage system references (u_{an_ref} , $u_{bn\text{-}ref}$) and ($u_{a'n\_ref'}$, $u_{b'n'\_ref}$) in an independent way. The architecture of the control system has been deduced from its CIOG by inversion (fig. 2). You can remark, that an indirect inversion (a closed-loop controller) is associated to a causal relation.

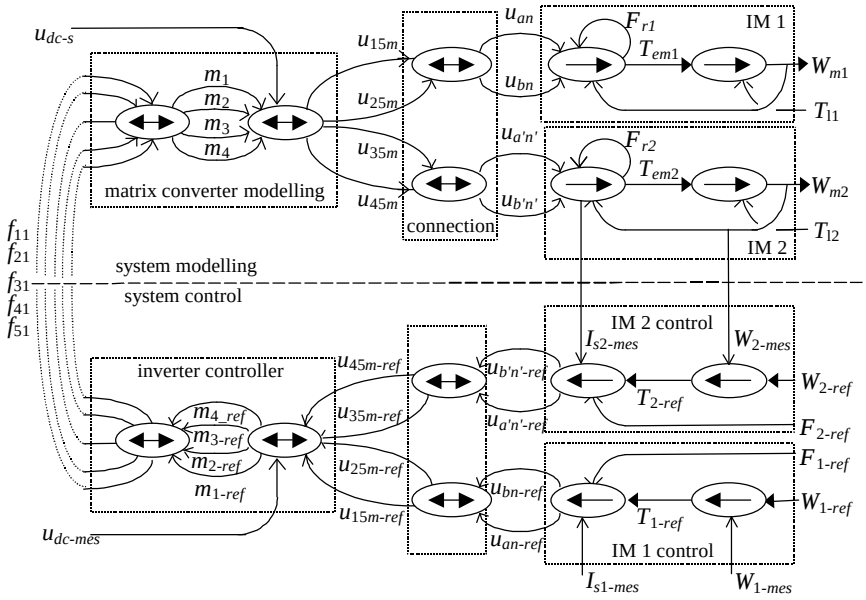

Fig. 2: CIOG of the power system control

An inverse transformation is necessary to obtain modulated voltage references from the knowledge of winding voltage references:

$$\begin{bmatrix} u_{15m-ref} \\ u_{25m-ref} \end{bmatrix} = 3 \begin{bmatrix} 2 & 1 \\ 1 & 2 \end{bmatrix} \begin{bmatrix} u_{an-ref} \\ u_{bn-ref} \end{bmatrix} \quad (7)$$

$$\begin{bmatrix} u_{35m-ref} \\ u_{45m-ref} \end{bmatrix} = 3 \begin{bmatrix} 2 & 1 \\ 1 & 2 \end{bmatrix} \begin{bmatrix} u_{a'n'-ref} \\ u_{b'n'-ref} \end{bmatrix} \quad (8)$$

References of conversion functions, $<m_{c\text{-}ref}>$, are obtained by linearisation with the measurement of the dc source voltage.

$$\left\langle m_{c-ref} \right\rangle = \frac{u_{c5-ref}}{u_{dc-mes}} \quad (9)$$

Corresponding switching references (switch states) are set by a connection controller which is presented in a sub-paragraph because of its originality.

3.2.- Modulation

3.2.1.- PPWM. The role of the pulse position and width modulator is to transform each mean conversion reference ($<m_{c\text{-}ref}>$) into an equivalent three level pulse (conversion reference, $m_{c\text{-}ref}$) with the same mean value during the modulation period (fig. 4). The pulse generation depends on two parameters:

- the mean conversion reference which induce the sign and the width of the conversion reference,
- the position of the pulse into the modulation period.

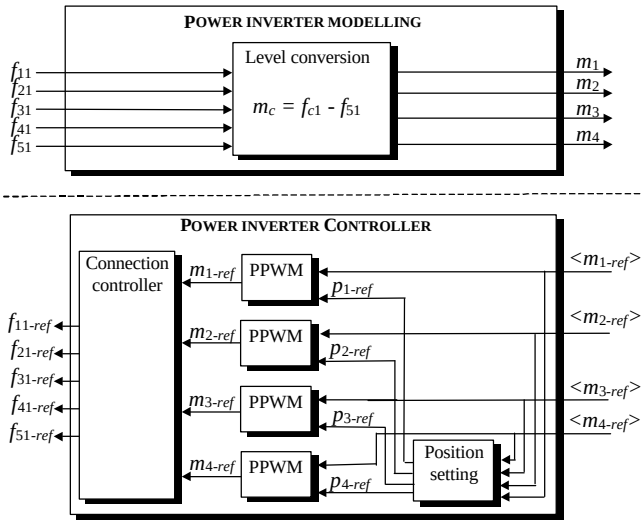

Fig. 3: Parallel PPWM

3.2.2.- Position setting by mixed modulation. At each modulation period, positions of pulse references must be set in order to create configurations from table 1. The position of the conversion function reference $m_{c\text{-}ref}$ will be noted $p_{c\text{-}ref}$.
In a previous paper [8], a separated modulation has been presented. It consists in separating the modulation period and, in each subdivided modulation period, each voltage system is separately modulated.

Here, a mixed modulation of both voltage systems is implemented inside the entire modulation period. From table

1, it can be shown that the four conversion functions must have the same sign at any time. It is a characteristic of matrix converters. Therefore, the sign of mean conversion function must be tested in order to create a subdivision of the time-variable conversion references in available configurations.

If all signs are identical, therefore a simultaneous and centered modulation of the four mean conversion function references is used (fig. 5).

$$p_{c-ref}\ (q.Tm) = \frac{1}{2}.\left(1 - \left|m_{c-ref}\ (q\ .\ Tm)\right|\right) \qquad (10)$$

Otherwise, a delayed modulation is implemented by setting position of positive conversion references to the left and negative level references to the right.

$$\text{If } \left\langle m_{c-ref}\ (q\ .\ Tm)\right\rangle \text{ is positive then } p_{c-ref}(q.Tm) = 0 \qquad (11)$$

$$\text{Otherwise } p_{c-ref}(q.Tm) = 1 - \left|m_{c-ref}\ (q\ .\ Tm)\right| \qquad (12)$$

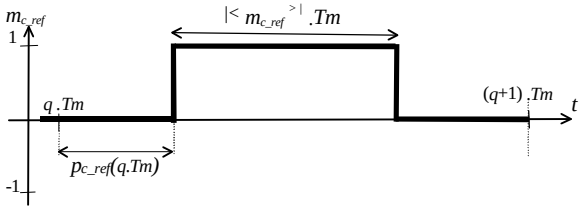

Fig.4: Conversion reference waveforms

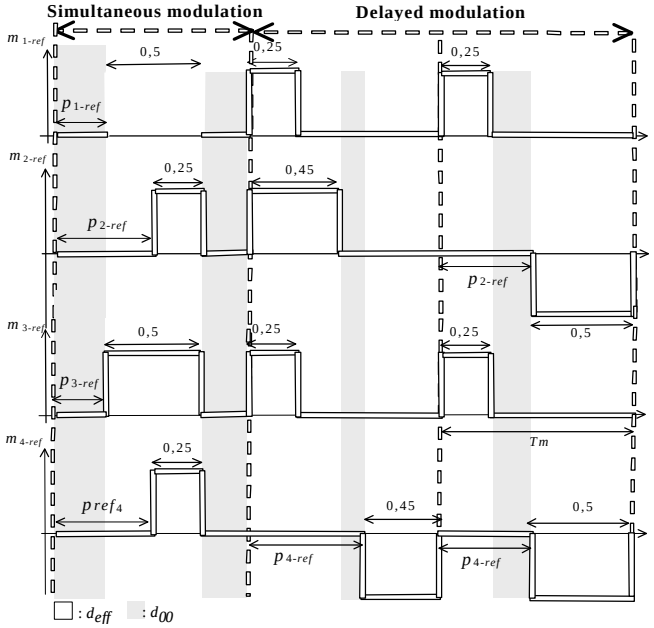

Fig. 5: Simultaneous and delayed modulation

3.2.3.- Null and effective conversions. During a modulation period, the conversion duration of electrical quantities is called "effective conversion duration". It depends on the used modulation and is defined as:

- $d_{eff} = max(|<m_{1\text{-}ref}>|,|<m_{2\text{-}ref}>|,|\ m_{3\text{-}ref}>|,|<m_{4\text{-}ref}>|).\ Tm$

for a simultaneous modulation, and

- $d_{eff} = max(|<m_{1\text{-}ref}>|,|<m_{2\text{-}ref}>|,|\ m_{3\text{-}ref}>|,|<m_{4\text{-}ref}>|).$
  $- min(|<m_{1\text{-}ref}>|,|<m_{2\text{-}ref}>|,|\ m_{3\text{-}ref}>|,|<m_{4\text{-}ref}>|)\ ).\ Tm$

for a delayed modulation.

Suppose, now that the operating points of induction machines requires two identical voltage systems in opposite sens (fig. 6):

$$<um_{15\text{-}ref}> = Uref_{max}\ .\sin(w\ .t)$$
$$<um_{25\text{-}ref}> = -\ Uref_{max}\ .\sin(w\ .t\ -\ 2\ .\pi\ /3) \qquad (13)$$

for the first one and

$$<um_{35\text{-}ref}> = -Uref_{max}\ .\sin(w\ .t)$$
$$<um_{45\text{-}ref}> = Uref_{max}\ .\sin(w\ .t\ -\ 2\ .\pi\ /3) \qquad (14)$$

for the second one. We get the following conversion references:

$$<m_{1\text{-}ref}> = Uref_{max}\ /\ u_{dc\text{-}s}\ .\sin(w\ .t)$$
$$<mr_{2\text{-}ref}> = -\ Uref_{max}\ /\ u_{dc\text{-}s}\ .\sin(w\ .t\ -\ 2\ .\pi\ /3) \qquad (15)$$
$$<m_{3\text{-}ref}> = -Uref_{max}\ /\ u_{dc\text{-}s}\ .\sin(w\ .t)$$
$$<m_{4\text{-}ref}> = Uref_{max}\ /\ u_{dc\text{-}s}\ .\sin(w\ .t\ -\ 2\ .\pi\ /3) \qquad (16)$$

by assuming $u_{dc\text{-}mes} = u_{dc\text{-}s}$.

At t=0.005 s, two sinusoidal conversion references have their extreme values with opposite signs. In consequence, a delayed modulation is required. The corresponding effective conversion duration has a maximum magnitude equal to:

$$d_{eff} = (2.\ Uref_{max}\ /\ u_{dc\text{-}s})\ Tm \qquad (17)$$

To be implemented, this duration must be lower than the modulation period and therefore we have the following constraint for the dc source voltage:

$$u_{dc\text{-}s} \geq 2\ Uref_{max} \qquad (18)$$

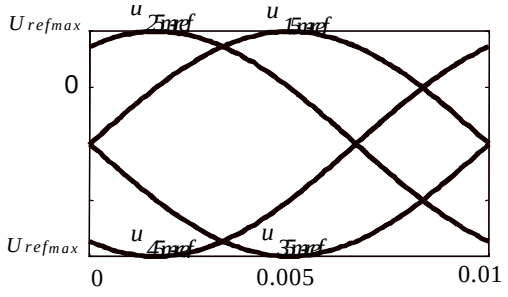

Fig. 6 : Waveforms of two opposite voltage reference systems

3.3.- Connection controller

The passage from switching functions f_{cl} to conversion functions m_c may be rewritten as the following matrix relation:

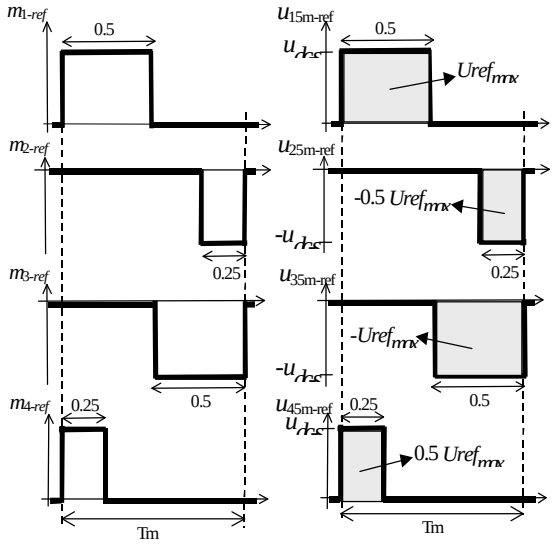

Fig. 7: Conversion reference waveforms

$$[E].[F] = [M].[N] \tag{21}$$

The connection controller paradigm consists to find the right switch states $[F_{ref}]$ in order to get the wished conversion references $[M_{ref}]$. As matrix $[E]$ and $[N]$ are not squared, no exact solution exists in linear algebra. A non-linear method has been used by determining in a first step the closest solutions given by a linear equation ($[F_{min\text{-}ref}]$). In a second step, a non-linear operator is applied in order to find the exact solution $[F_{ref}]$. The set of minimal solutions may be expressed as :

$$\lfloor F_{min-ref} \rfloor = \lfloor F_{M\text{-}ref} \rfloor + \lfloor F_{H\text{-}ref} \rfloor \tag{22}$$

* $[F_{M\text{-}ref}]$ represents the contribution of conversion functions:

$$\left[F_{M-ref}\right] = [E]^{\mathrm{T}}\left([E][E]^{\mathrm{T}}\right)^{-1}\left[M_{ref}\right][N] \tag{23}$$

$$\begin{bmatrix} f_{M11-ref} & f_{M12-ref} \\ f_{M21-ref} & f_{M22-ref} \\ f_{M31-ref} & f_{M32-ref} \\ f_{M41-ref} & f_{M42-ref} \\ f_{M51-ref} & f_{M52-ref} \end{bmatrix} = \frac{1}{5}\begin{bmatrix} 4 & 1 & -1 & -1 \\ -1 & 4 & -1 & -1 \\ -1 & -1 & 4 & -1 \\ -1 & -1 & -1 & 4 \\ -1 & -1 & -1 & -1 \end{bmatrix}\begin{bmatrix} m_{1-ref} \\ m_{2-ref} \\ m_{3-ref} \\ m_{4-ref} \end{bmatrix}\begin{bmatrix} 1 & -1 \end{bmatrix} \tag{24}$$

* $[F_{Href}]$ represents the repartition of short circuits over the switch matrix. If we set null all conversion function references ($[M_{ref}]=[0]$), we obtain:

$$\lfloor F_{min-ref} \rfloor = \lfloor F_{Href} \rfloor \tag{25}$$

$$\left[F_{Href}\right] = \left([I] - [E]^{\mathrm{T}}\left([E][E]^{\mathrm{T}}\right)^{-1}[E] \right)\left[H_{ref}\right]$$

* $[I]$ is an unity matrix

* $[H_{ref}]$ is a matrix with the same size of $[F]$

$$\begin{bmatrix} f_{H11-ref} & f_{H12-ref} \\ f_{H21-ref} & f_{H22-ref} \\ f_{H31-ref} & f_{H32-ref} \\ f_{H41-ref} & f_{H42-ref} \\ f_{H51-ref} & f_{H52-ref} \end{bmatrix} = \frac{1}{5}\begin{bmatrix} x & (1-x) \\ x & (1-x) \\ x & (1-x) \\ x & (1-x) \\ x & (1-x) \end{bmatrix} \tag{26}$$

* $x \hat{I} \{0,1\}$

The exact solutions may be found by applying a non-linear operator on each found minimal solution. The step function has been chosen in order to generate binary values:

$$\begin{aligned} \mathrm{POS}(x) &= 1 \text{ if } x>0 \\ \mathrm{POS}(x) &= 0 \text{ otherwise.} \end{aligned} \tag{27}$$

$$\lfloor F_{ref} \rfloor = POS\left(\lfloor F_{Mref} \rfloor\right) + POS\left(\lfloor F_{Href} \rfloor\right) \tag{28}$$

It can be easily shown, that the first term of this last expression implements effective conversion patterns (patterns 2 to 31 in table 1) and the second term implements null conversion patterns (pattern 1 and pattern 32). More over, when setting null conversion patterns, if x=1, all switching functions of the first line are closed. If x=0, all switching functions of the second line are closed in order to implement $[M_{ref}]=[0]$. Minimization of switch commutation is possible through this parameter.

4.- SIMULATION RESULTS

Significant results are now presented. The d.c. voltage value has been set to $u_{dc\text{-}s}$ = 127.√2.√3.2 = 1080 V and the modulation frequency to 5 kHz. The speed of both machines is set to 1000 rpm in opposite sense.

4.1.- Winding voltages

As expected, the obtained winding voltages have a rms value of 220V (fig. 8). This is mainly the consequence of the perfect control of modulated voltages as it is shown on the frequency spectrum.

4.2.- Switching states

The frequency analysis of switching functions shows the presence of a d.c. ray, a 50Hz ray, a 150 Hz ray and a ray family around the modulation frequency (fig. 9).

4.3.- Mechanical performances

Dynamic performances of the torque and speed control have been also tested. Figure 10 presents the obtained simultaneous speed responses to particular simultaneous reference trajectories. As noted, both machines have really independent speeds.

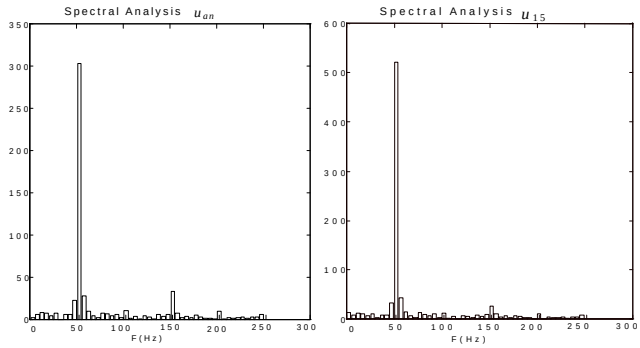

Fig. 8: Frequency spectrum of voltages

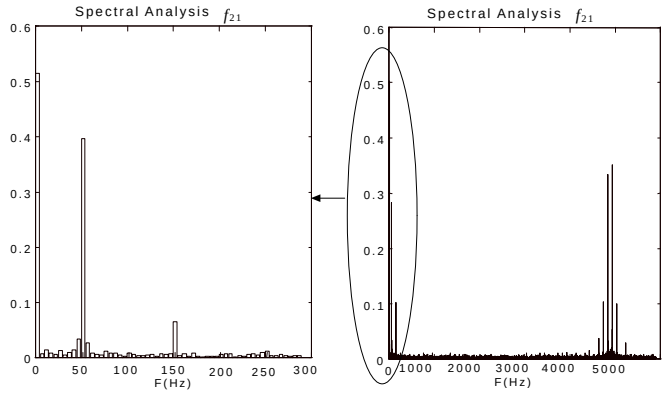

Fig. 9: Frequency spectrum of f_{21}

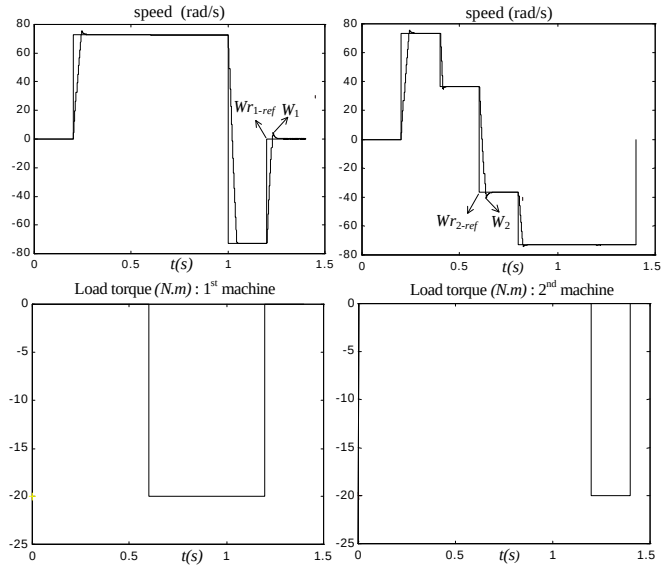

Figure 10: Trajectories of both ac machines

Frequencies and magnitude of the two current systems are different as speeds and torques are different, sinusoidal evolution is assessed (fig. 11).

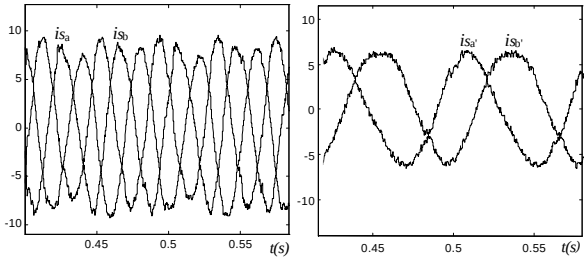

5.- CONCLUSION

A specific control of an original five-phase inverter has been presented in order to supply two induction machines. In order to obtain the maximum voltage rate, a PPWM is developed. If the power switch number is reduced, the voltage source must be increased in order to keep the same performance of both machines. The theoretical strategies lead to impose independent behaviours on both machines even if a commutation cell is in common.

References

[1] J.M. Barnard, J.D. Van Wyk, W.G. Dunford: Battery operated wheelchairs using three-phase cage rotor induction machines and PWM inverters, EPE Journal, Vol. 4, n°1, March 1994, pp 15-19.

[2] B. Wu, S.B. Dewan : A modified current-source inverter for a multiple induction motor drive system, IEEE Trans. on Power Electronics, Vol. 3, n°1, January 1988, pp 10-16.

[3] R.D. Lorentz, T.A. Lipo, D.W. Nowotny: Motion control with induction motors, Proceeding of the IEEE, Vol. 82, n° 8, August 1994, pp 1215-1240.

[4] A. Bouscayrol, M. Pietrzak-David, B. De Fornel: Comparative studies of inverter structures for a mobile robot asynchronous motorisation, Proceeding of ISIE Conference, Warsaw, Poland, June 1996, pp 447-452.

[5] J. P. Hautier, J. Faucher: Le graphe informationel causal, Bulletin de l'Union des Physiciens, vol. 90, juin 1996, pp 167-189.

[7] W. Leonhard: 30 years space vectors, 20 years field orientation, 10 years digital signal processing with controlled ac. drives, EPE Journal, vol. 1, n° 1, July 1991, pp. 13-20.

[8] B. François, A. Bouscayrol: Design and modelling of a five phase voltage source inverter for two induction motors, Proceeding of EPE'99, Lausanne, Switzerland, 7-9 Sept. 1999.